Transactions of the **14th International Conference on Structural Mechanics in Reactor Technology** (SMiRT 14), Lyon, France, August 17-22, 1997 **F04/5**

Experiment and numerical analysis of a typical nuclear piping submitted to large cyclic thermal shocks

Geyer P.
EDF, France

ABSTRACT : A mock-up composed of some nuclear power plants components has been submitted to large thermal shocks on a test loop. The purpose of these tests was to verify the inoffensiveness of ratchetting for such loadings and to study the conservatism of design rules. For piping components which no longer check the design rules, numerical simulations could be an alternative method of analysis. One of the piping tested on the test loop is used to evaluate the performance of constitutive models in predicting thermal ratchetting.

1. INTRODUCTION

With the new operating conditions of PWR French reactor, some piping auxilliary components of the reactor coolant system no longer check the RCC-M criterion with regard to the risk of progressive deformation. Therefore, R&D actions were initiated by Framatome, CEA and EDF [1] in 1991-1992 with the aim of putting forward more suitable design criteria than the present rules, which seem to be too conservative. In a first program [2], CEA has realized a parametric study on a mock-up to determine the thermomechanical conditions to obtain ratchetting.

This paper deals with a second program on the pressurizer auxilliary spray line of Pressurized Water Reactor (PWR) nuclear power plants. This line may be submitted to severe temperature transcients during upset conditions : a 325°C cold thermal shock in one second (from 345 to 20°C) is followed by a 200°C hot thermal shock (from 20 to 220°C). For such transcients, the RCC_M French design code rules that prevent ratchetting deformation hazard are not respected for some components with thickness transition. EDF has realized twenty thermal cycles under internal pressure of 15.8 MPa on a representative mock-up (Fig. 1 & 2) composed of some piping (2'' pipes, 6 ''x2''x6'' T-piece...). During these tests, many temperature, strain and diametral variations were measured. Ratchetting detected on some components, is a weak progressive diameter increase during a few cycles [3]. These experimental results have been already used to study the conservatism of design rules [4]. Numerical simulations could be an alternative method of analysis [1]. Results on a monobloc pipe with a reinforcement (see geometry on Fig. 3) are used to evaluate the performance of Chaboche and Burlet&Cailletaud model [5,6] in predicting thermal ratchetting.

2. CONSTITUTIVE MODELS' DESCRIPTION

Given the temperatures seen during the test, the time-dependent effects are disregarded, and an elastoplastic model is considered. Problem is seen in the context of small strains and therefore the strain tensor ε is additively decomposed into an elastic part and a plastic part : $\varepsilon = \varepsilon^e + \varepsilon^p$. In order to define the yield surface, conventionally a Von Mises criterion is used in which kinematic and isotropic strain hardening are introduced (translation and dilation of the plasticity surface).

It is well known that modelling of ratchetting is strongly influenced by the kinematic hardening rule adopted. It has been shown, that the Armstrong & Frederick kinematic hardening rule used in Chaboche model leads to a broad overestimation of ratchetting in tension-torsion tests conducted on 316L stainless steel specimens [5]. Burlet & Cailletaud proposed [6], a non-linear kinematic hardening rule with radial evanescence in order to improve the description of multiaxial ratchetting. For tension-torsion tests, it is easy to show analytically the advantage of coupling the A-F kinematic hardening rule and those proposed by Burlet & Cailletaud [7]. This is also the way adopted in the present study: the set of equations used to describe isotropic (eq.1) and kinematic hardening (eq. 2) is given below. These constitutive equations called A-F & B-C model in this paper, are identical to that of Chaboche model under radial loading or when parameters δ_1 and δ_2 are equal to 1. Therefore, these two parameters may be identified independently with 2D ratchetting tests.

$$\dot{R} = b\left(R_\infty - R\right)\left\|\dot{\varepsilon}^p\right\| \text{ with } R(0) = R_0 \tag{1}$$

$$\begin{cases} \mathbf{X} = \mathbf{X}_1 + \mathbf{X}_2 \quad \text{with} \quad \dot{\mathbf{X}}_i = C_i\left(2/3\, a_i\, \varphi(p)\, \dot{\varepsilon}^p - \left(\delta_i\, \mathbf{X}_i + (1-\delta_i)(\mathbf{X}_i : \mathbf{n})\,\mathbf{n}\right)\left\|\dot{\varepsilon}^p\right\|\right) \\ \varphi(p) = 1 + (\psi - 1)\exp(-\omega\, p) \end{cases} \tag{2}$$

where $\left\|\dot{\varepsilon}^p\right\|$ is the equivalent cumulated plastic strain rate and $\mathbf{n}$ the normal of the yield surface.

3. MATERIAL PARAMETERS' IDENTIFICATION

To identify the material parameters, a specific characterization program was undertaken on specimens machined in the same material that the monobloc pipe with a reinforcement tested (SS 304L). This program included :

- monotonic tensile tests,

- cyclic uniaxial tension-compression tests (oligocyclic fatigue tests) for half amplitude strain ranges $\Delta\varepsilon/2$ between 0.15 and 1.5 % ,

- tension-torsion ratchet tests for 2 values of tensile stress (50 Mpa and 100 Mpa) and increasing shear amplitudes ($\Delta\varepsilon_{\theta z}/2$ = 0.15, 0.30 then 0.45%).

All these tests were performed at 20, 220 and 350°C.

Material parameters' identification was performed for the three temperatures with the help of the software SiDoLo (optimization program) [8]. Parameters values obtained are given in table 1.

Fig. 5 show a comparison between experiments and simulations of the monotonic tensile curves and the cyclic curves obtained for uniaxial loading tests. On the Fig. 6, predictions of some tension-torsion tests at 220°C are given for the Chaboche model ($\delta_1 = \delta_2 = 1.$) and for the A-F & B-C model ($\delta_1 = 1.$ and $\delta_2 = 6.10^{-4}$). This figure shows the broad overestimation of the ratchetting with the Chaboche model. It was thus shown that satisfactory modelling of the characterisation tests was obtained with the A-F & B-C model.

T (°C)	E	ν	R_0	R_∞	b	k	ω	a_1	a_2	C_1	C_2	δ_1	δ_2
20°	197000	0.31	158.	158.	0.	0.93	4.	127.5	110.	187.	5150.	1.	1.10^{-4}
220°	183000	0.31	134.	134.	0.	0.7	5.	155.5	35.	322.	3264.	1.	1.10^{-4}
350°	160000	0.31	122.	122.	0.	0.6	4.	122.	50.	400.	5480.	1.	1.10^{-4}

Table 2 : Coefficients of the Burlet model (units : MPa, s) - A 304L

4. NUMERICAL ANALYSIS OF THE MONOBLOC PIPE WITH A REINFORCEMENT

Due to the welding and the discontinuity between the 2 pipes, modelization of the socket-welding mentionned on Fig. 1 is a difficult task with large uncertainties. This is the reason why a monobloc pipe with the same geometry is put on the mock-up tested on the test loop.
The mock-up is submitted on CUMULUS facility to 20 thermal cycles under an internal pressure of 15.8 Mpa. The model is initially heated to 345°C. At this point, 20°C cold water is injected in the mock-up with a 15 m^3/h flow during 53 seconds (Fig. 2). Then 250°C hot water is made to circulate in the mock-up with at first a 13 m^3/h flow during 3 minutes and then with a 9 m^3/h flow during 9 minutes. Then the model is isolated and heated to 345°C.
The experimental measurement obtained in the thick part of the pipe are given on Fig. 7 (see Fig. 4 for thermocouple position). These results show that the cold shock of 325°C lasts 1 second and the warm thermal shock of 230°C lasts 80 seconds.
For the monobloc pipe studied, experimental results in terms of ratchetting concern only internal diametral measurements in three places named A, B and C on Fig.3, before and after the first cycle and after the twenty cycles. Results given in Table 2 show that internal diameter variations ($\Delta\phi_{int}$) are very small (from 20 to 50μm).

Position (mm)	1st cycle	20th cycle
C (d=47)	20 ±4	31±4
A (d=111)	23±4	36±4
B (d=178)	38±4	51±4

Table 2 : Inner diameter variation : $\Delta\phi_{int}$ (μm) - measurements

A FE mesh with 607 quadratic axisymmetric elements (Fig. 4) is used to analyse the monobloc pipe with a reinforcement.
Thermo-mechanical calculations were performed using the Chaboche and A-F & B-C model over 5 loading cycles with the finite element code *Code_Aster*© developed at EDF. Plastification occurs during the cold and the warm shocks. The cumulated plastic strain is maximum near the place named B on Fig.3.

In terms of displacement, results obtained with the two models are similar and near experimental measurements at the end of the first cycle (Fig. 8). After 5 cycles, ratchetting deformations induced by the two models are close together with some differences : radial displacement is higher in the thick part ($z \cong 100$ mm) with Chaboche model and higher near the thickness transition ($z \cong 60$ mm) with A-F & B-C model. These results appear to contradict the predictions of tension-torsion tests obtained with the two models. To understand this point, we have considered the plastic strain vs stress curves obtained by both models (Fig. 11) where the cumulated plastic strain is maximum (near B). These curves show that low plastic strain amplitudes values (between 0.15 and 0.4%) are obtained. Results obtained by both models are similar for hoop components, but a great difference is obtained for axial components. This difference occurs during the warm shock (compressive plastification). Because the differences between the two models consist in the writting of the kinematic hardening evolution laws, we have considered values of the kinematic hardening variables at the same place. With identification results for A-F & B-C model ($\delta_1 = 1.$ and $\delta_2 = 1.10^{-4}$), loading paths obtained for the first kinematic hardening variable (X1) are similar for both models. For the second kinematic hardening variable (X2), loading paths are given on Fig.12 : stabilized loops are obtained with Chaboche model and abnormal evolution with A-F & B-C model. That means that improvement obtained with kinematic hardening rule proposed by Burlet & Cailletaud in the case of tension-torsion test can lead to bad simulations for other kinds of loadings. With recent tests in tension-torsion carried out with bowtie type loading combining simultaneous cycling of axial stress and shear strain, we have shown [9] that A-F & B-C model can produce more ratchetting than Chaboche model.

In order to compare the experimentals results with FE results, the extrapollation rule proposed in RCC-MR [10] is used to evaluate the radial displacement at 20 cycles (Fig. 9). A slight underestimation is obtained with Chaboche model. The ratchetting rate obtained with A-F & B-C model at place named A is too large.

5. CONCLUSIONS

In order to study the conservatism of RCC-M criterion with regards to the risk of progressive deformation, some experiments have been realized by EDF and CEA [2,3]. These tests are used to evaluate the performance of constitutive models in predicting thermal ratchetting [this issue, 10]. With FE analysis of a typical nuclear piping submitted to large thermal shocks, we show that kinematic hardening rule proposed by Burlet & Cailletaud to improve the modelling of ratchetting in tension-torsion test can lead to bad simulations for more complex situations. It means that simple ratchet tests as tension-torsion tests are not representative of ratchetting with more complex loadings. Another interesting result of this study is that Chaboche model doesn't lead necessary to a large overestimation of ratchetting.

These models have also been used in the frame of a benchmark on tests conducted at CEA on straight pipes with an abrupt change in thickness which were subjected to a constant internal pressure and cyclic heating by Joule effect. The modifications of kinematic hardening rules with the notion of critical state (as proposed by Ohno & Wang) lead to more strongly build models [10].

REFERENCES

1. Pellissier-Tanon, A. et al. 1993. Alternative methods for PWR primary piping analysis induced by operating experience. *Proc. SMIRT 12:* Vol. DF: 389-400, Stutgart (Deutchland).

2. Cabrillat, M. T. & MEZIERE, Y. 1997. Evaluation of ratchetting on experimental tests using simplified design rules. *Proc. SMIRT 14:* Vol. F, Lyon (France).

3. Couterot, C., & E. Fetet 1993. Compte rendu des essais sur Cumulus de la maquette déformation progressive soumise à des chocs thermiques de forte amplitude. EdF report HT/26/93/03 5/A.

4. Couterot, C., P. Geyer & J. M. Proix 1994. Experiment and numerical analysis of the NPP pressurizer auxilliary spray line submitted to large thermal shocks. *Proc. PVP.* Minneapolis.

5. Chaboche, J. L., 1991. On some modifications of kinematic hardening to improve the description of ratchetting effects. *International Journal of Plasticity* 7: 661-678.

6. Burlet, H. & G. Cailletaud 1987. Modeling of cyclic plasticity in finite element codes. *Proc. 2nd Int. Conf. on Constitutive Laws for Engineering Materials.* Tucson, Arizona.

7. Geyer, P. 1995. On use of radial evanescence remain term in kinematic hardening. *Proc. SMIRT 13:* Vol. L: 699-705, Porto-Allegre (Brasil).

8. Pilvin, P. 1988. Identification des paramètres de modèles de comportement. *Proc. MécaMat'88*: 155-164. Besançon (France).

9. Portier, L., S. Calloch, P. Geyer & D. Marquis 1997. Cyclic plasticity investigations including ratchetting and hardening under nonproportional loadings. Experiments and modelling. *Proc. SMIRT 14:* Vol. L, Lyon (France).

10. Cabrillat, M. T. et al. 1997. Benchmark on a thermal ratchetting test. Comparison of different constitutive models. *Proc. SMIRT 14:* Vol. L, Lyon (France).

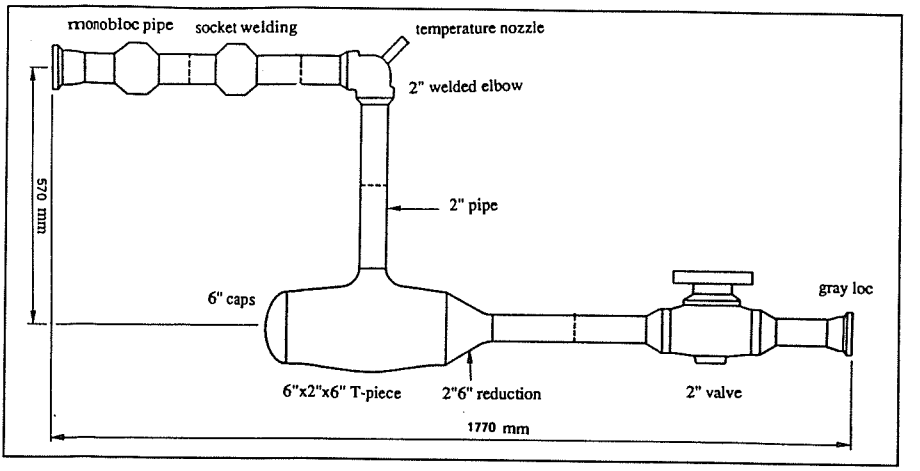

Figure 1: Mock-up shematic

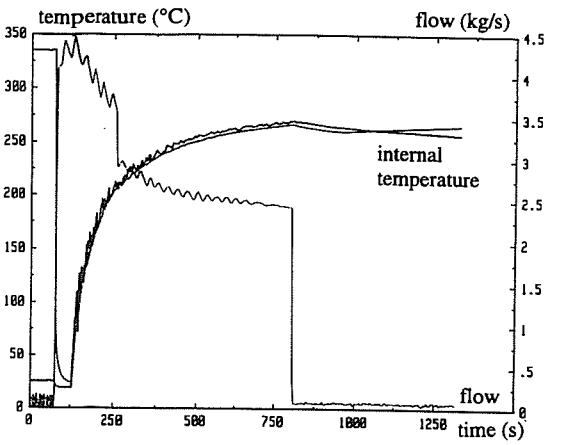

Figure 2: Thermal transient on the test loop

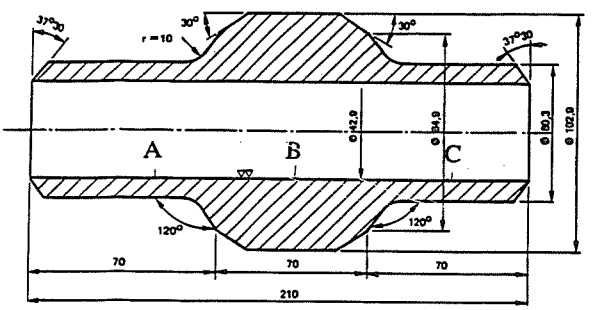

Figure 3: Monobloc pipe geometry

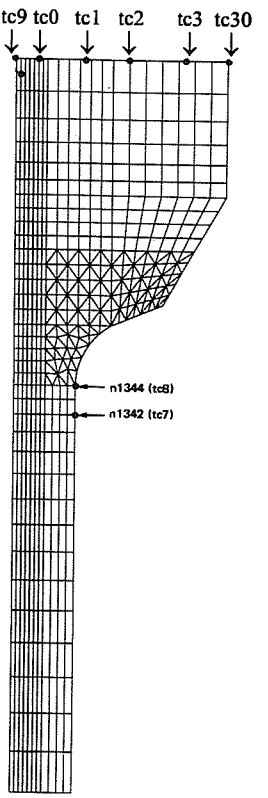

Figure 4: Monobloc pipe mesh

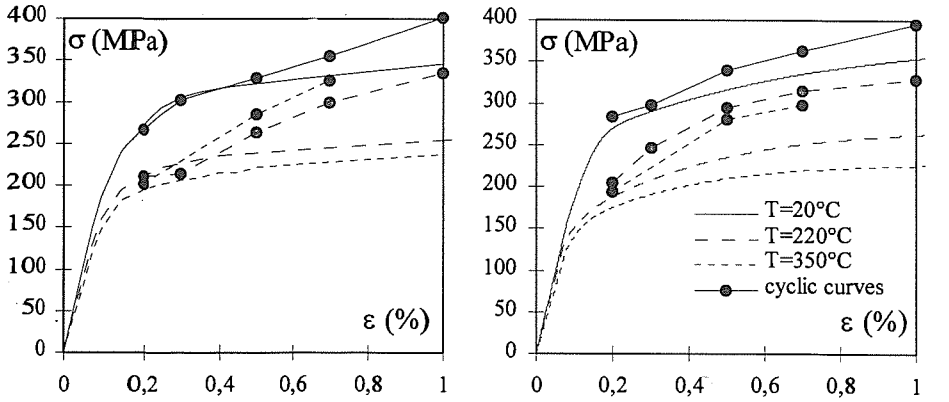

(a) Experiments. (b) Predictions.

Figure 5: Monotonic and cyclic curves at 20, 220 and 350°C.

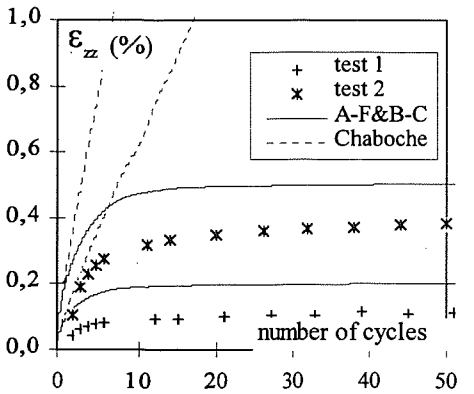

Figure 6: Ratchetting in tension-torsion tests (σ_{zz} = 50 and 100 MPa, $\Delta\varepsilon_{\theta z}/2$ = 0.15%) at 220°C.

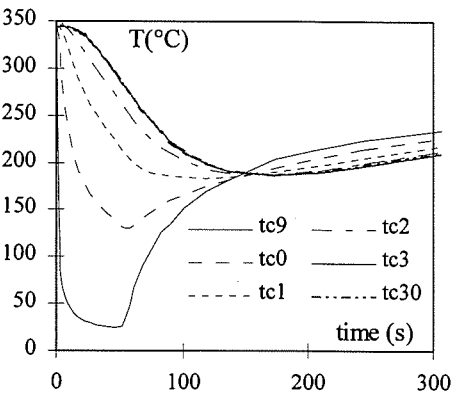

Figure 7: Temperature-time curves in thick part of the pipe

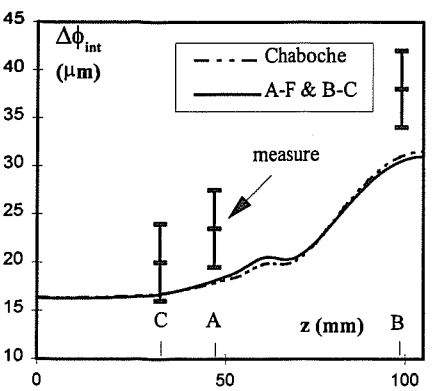

Figure 8: Internal diameter variations along the pipe at the end of the first cycle.

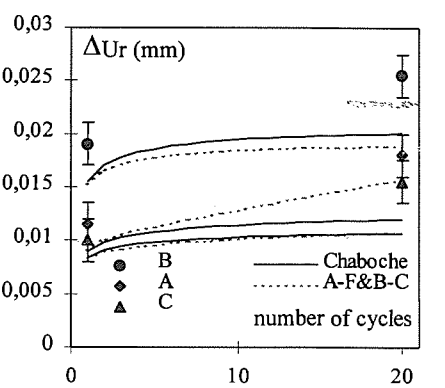

Figure 9: Evaluation at the 20th cycle of internal radial displacement at point A,B,C.

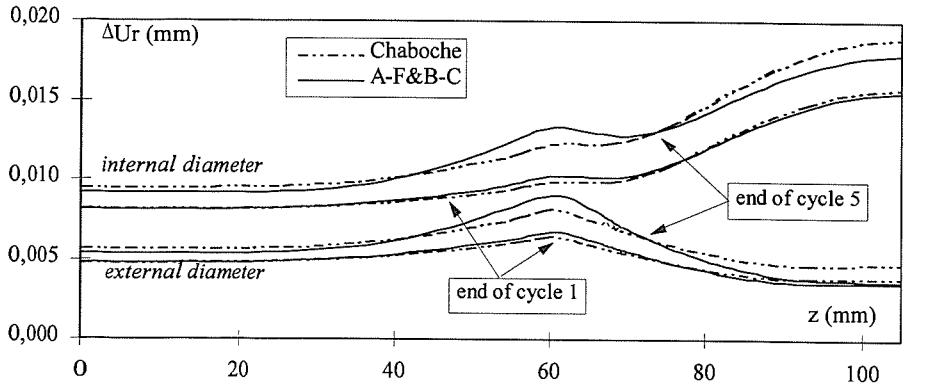

Figure 10: Radial displacement along the internal and external diameters

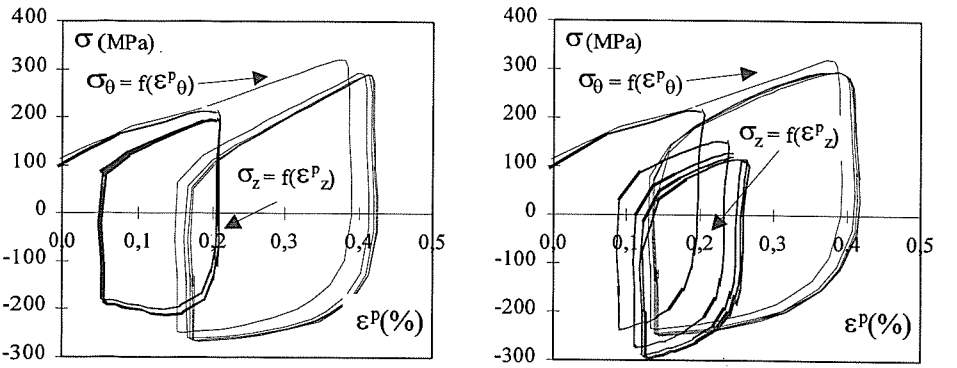

(a) analysis with Chaboche model (a) analysis with A-F & B-C model

Figure 11: Plastic strain versus stress at node where the cumumated plastic strain is maximum (near B)

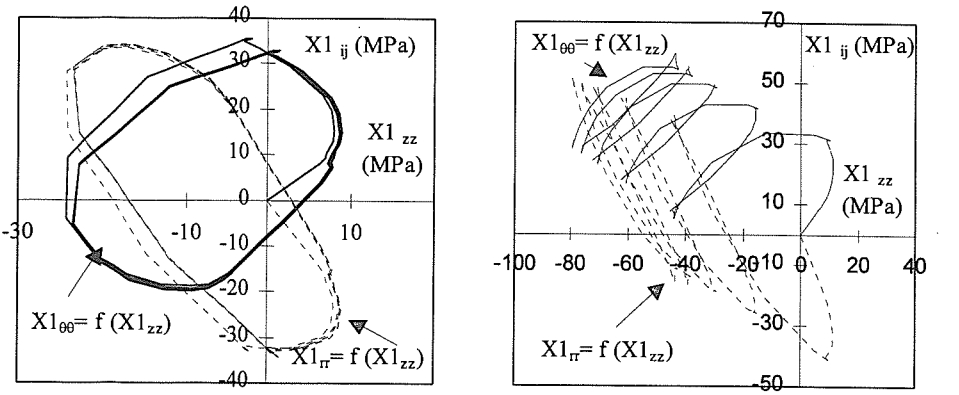

(a) analysis with Chaboche model (a) analysis with A-F & B-C model

Figure 12: Kinematic hardening loading paths (near B).